AIAA Aviation Forum and ASCEND co-located Conference Proceedings
29 July - 2 August 2024, Las Vegas, Nevada
AIAA AVIATION FORUM AND ASCEND 2024
10.2514/6.2024-4420

Design and Testing of Deflected Slipstream Airfoil for VTOL Hover Enabled by CoFlow Jet

Gecheng Zha [*], Yan Ren [†]
CoFlow Jet, LLC
4649 Ponce de Leon Blvd., Suite 306, Coral Gables
FL 33146, USA

William Fredericks [‡]
1100 Exploration Way Suite 302S
Hampton, VA 23666

Abstract

This paper reports a design and testing research work to demonstrate the performance of a Deflected Slipstream (DS) airfoil for VTOL hover, which is enabled by CoFlow Jet (CFJ) active flow control. A CFJ-NACA-6421 airfoil with a chord of 65 cm is designed and tested. The flap has 66.74%C with 4 Schubeler EDF DS-30-AXI (69 mm) fans used as CFJ actuators. The aerodynamic design includes the flapped CFJ airfoil with optimized injection and suction location and size, internal ducts, and matching the micro-fans as the CFJ actuator. The test was conducted using a frame to hold the airfoil section in outdoor environment to mimic static hover condition. The testing includes measuring lift and drag, which are used to calculate the flow deflection angle. Flow visualization with smoke and tufts were used to observe the slipstream deflection. The airfoil setup has the flap deflected upward to avoid ground effect. The deflected slipstream enabled by CoFlow Jet is proven to be very effective by both the force measurement and flow visualization. The slipstream deflection angle θ is always greater than the flap deflection angle β. For as low as a flap deflection angle of 78°, the slipstream can be deflected to 90° - 120°. A deflection angle of more than 90° will generate backward thrust.

Nomenclature

A	Propeller disk area
AR	Wing aspect ratio
AoA	Angle of attack
CFJ	Co-flow jet
C	Profile chord
C_L	Lift coefficient $L/(q_\infty S)$
C_D	Drag coefficient $D/(q_\infty S)$
C_m	Pitching moment coefficient $M_{c/4}/(q_\infty Sc)$
C_μ	Jet momentum coef. $\dot{m}_j U_j/(q_\infty S)$
$(C_L/C_D)_c$	CFJ airfoil corrected aerodynamic efficiency $C_L/(C_D + P_c)$
$(C_L^2/C_D)_c$	CFJ airfoil corrected productivity efficiency $C_L^2/(C_D + P_c)$
D	Drag
DS	Deflected Slipstream
DL	Disk loading, thrust of the actuator disk/actuator disk area

[*] Ph.D., President, AIAA Associate Fellow, Professor, U. of Miami
[†] Ph.D., CTO
[‡] CTO, Chairman

DL_c	Disk loading coefficient
FM_{DS}	Figure of Merit for the DS system
L	Lift
LE	Leading Edge
M	Mach number
P_{tot}	Total power of the DS-CFJ system
P_c	CFJ power coefficient $P/(q_\infty S V_\infty)$
P_P	Propeller actuator power coefficient $\frac{2}{\rho V_\infty^3 S}\sqrt{\frac{F^3}{2\rho A}}$
PL	Power loading, power/lift
PL_c	Power loading coefficient
ΔP	Pressure percentage increase across the propeller actuator disk
p	Static pressure
q	Dynamic pressure $0.5\,\rho U^2$
R	Propeller disk radius
S	Wing planform area
T	Thrust
TE	Trailing Edge
U	Flow velocity
$_j$	Jet conditions
δ	Flap deflection angle, deg
β	Resultant force angle of the DS-CFJ system about horizontal
$d\beta$	Resultant force angle variation range
ρ	Air density
$\dot{m}$	Mass flow
Γ	Total pressure ratio of the CFJ injection to suction
∞	Free stream conditions

1 Introduction

Vertical takeoff and landing aircraft is an important area of aviation for their special features of independence from runways. The current development of urban air mobility enhances the demands of advanced VTOL technologies. Electric vertical takeoff/landing (eVTOL) [1] fixed wing aircraft are playing a critical role in the transformation of urban transportation and eCommerce goods shipment. The current first generation (1G) eVTOL technology is based on conventional rotorcraft aerodynamic principles with vertical propellers facing upward for hover, including tiltrotors (e.g. V-280, V-22, Joby), tiltwings (e.g. Hiller X-18, Airbus Vahana18), and lift-plus-cruise (e.g. SB-1, Wisk). The 1G eVTOL does have a significant advantage over conventional rotorcraft by using distributed propulsors of multiple small propellers, which benefit noise mitigation, increase efficiency, and enable higher cruise speed using fixed wing configurations.

Conventional rotorcraft technology uses vertical propellers to lift up vehicles by exhausting flow downward (downwash), which has high hover efficiency. However, if the air vehicle requires a forward flight mission, a vertical propeller would have the disadvantage of low cruise efficiency. In general, rotorcraft have the following three limitations: 1) High complexity: A tiltrotor or tiltwing must be used to rotate the propellers to face forward direction. Such a system needs a complex mechanical system with high weight penalty. A complex system may be more prone to reliability issues. Transition between hover and cruise could also pose a challenge as it must ensure sufficient lift and trim when the full cruise speed is not yet achieved (takeoff) or is aborted (landing). 2) Noise: The noise level at cruise could be controlled by reduced disk loading and rotor tip speed. However, the broadband noise generated at hover due to flow separation caused by the rotor downwash-wing interaction and its turbulent wakes is significant and difficult to avoid. 3) Range: A rotorcraft based VTOL vehicle in general has low

mission efficiency that affects the range. This is due to their weight and drag penalty associated with some major components only used for hover instead of the entire flight envelop, such as the lift-plus propellers/struts and the heavy rotor or wing tilting system.

The motivation of this paper is to demonstrate an effective deflected slipstream technology enabled by CoFlow Jet active flow control, which has the potential to improve VTOL aircraft mission efficiency and mitigate hover noise by avoiding using conventional vertical rotor lifting principle.

1.1 Deflected Slipstream VTOL

The Deflected Slipstream (DS) concept pioneered by Kuhn and Draper in NACA in the late 1950's [2–4] generates hover lift by deflecting the slipstream from the propeller downward using a deflected flap. Once airborne, the flap is retracted for high-speed cruise. Fig. 1 illustrates the concept of Kuhn and Draper [3]. An effective DS wing system would not need to use tiltwings, tiltrotors or lift-plus configurations to simplify the system.

The deflected slipstream concept can be explained by a control volume analysis based on the sketch in Fig. 2, which illustrates a running propeller and a flapped airfoil immersed in a static field enclosed by a rectangle control volume with two horizontal boundaries and two vertical boundaries. The far field boundaries are far enough that the velocity is zero except at the lower boundary, which has a slipstream deflected by the flap exciting the boundary at an averaged velocity $\mathbf{V_{DS}}$ and flow angle β about the horizontal. Applying fluid mechanics momentum equation on the control volume with a simply connected domain surrounding the airfoil will give,

$$\mathbf{F} = \iint_s (\rho \mathbf{V} \cdot d\mathbf{S})\mathbf{V} = -\dot{m}\mathbf{V_{DS}} \tag{1}$$

where $\mathbf{F}$ is the resultant force acting on the airfoil, ρ and $\mathbf{V}$ are the flow density and velocity on the control volume boundaries respectively, and $\dot{m}$ is the mass flow of the slipstream crossing the lower boundary. Eq. (1) means that the resultant force acting on the airfoil is in the opposite direction of the deflected slipstream velocity $\mathbf{V_{DS}}$. If $\beta \neq 90°$, the airfoil has a lift and thrust (or drag) component. If β is 90°, the resultant force $\mathbf{F}$ becomes all lift. This is how the DS system generates the lift without tilting the rotor, but by deflecting the flap. Eq. (1) indicates that increasing the deflected slipstream mass flow and velocity will increase the resultant force. For vertical takeoff and landing hover maneuver, it is desirable to have $\beta = 90°$, but a range such as $\beta = 90° \pm d\beta$ with $d\beta < 10°$ may also function with typical surrounding environment. For cruise, the propeller generates thrust with $\beta = 0°$. The variation between lift and thrust for a DS system is controlled by varying the deflection angle of the flaps.

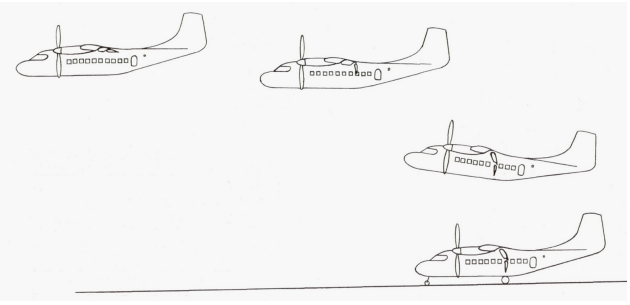

Figure 1: VTOL based on a deflected slipstream system [3].

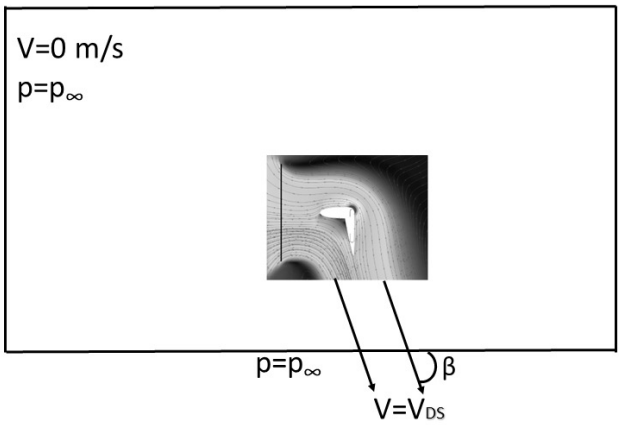

Figure 2: Control volume analysis of a deflected slipstream system.

The deflected slipstream principle seems simple and clear, but turning the horizontal slipstream from the propeller vertically downward is very challenging because flow suffers severe separation when the flap angle is large. A double-plain flap system tested by Kuhn and Draper [2] was able to deflect the flow by

45°. A double-slotted flap [3] increased the deflection to 63°. Such a flow deflection is not sufficient for hover, in particular with the ground effect. The efforts using DS for VTOL were abandoned in 1960's. Antcliff et al at NASA [1] recently revisited the DS concept and suggested using CoFlow Jet (CFJ) active flow control (AFC) to enhance the flow turning. They envision that it "could provide benefits in cruise efficiency, weight, noise, reliability, and maintainability, and offer safer transition characteristics" [1].

It is appealing if the CoFlow Jet AFC can achieve the following three features: 1) turn the slipstream 90° with fully attached flow; 2) have low energy expenditure that a DS-CFJ achieves a similar hover efficiency to a vertical rotor; 3) increase the cruise efficiency. The third feature is addressed in [5–10] for regular CFJ airfoils with the injection slot closer to the airfoil leading edge. The second feature needs more accurate measurement with a well designed system. It will be left as a future work. Zha studied it conceptually in a 2D simulation and shows it is promising. This paper is to focus on addressing the feasibility of the first feature. Such a DS VTOL system would have all the major components used in entire flight envelop including hover, climb, cruise, and extreme maneuver, instead of being only used at one point of the flight envelop. It would reduce weight and enable a high mission efficiency. It would also avoid the hover downwash interaction with the aircraft wings and fuselage to mitigate the broad band noise caused by flow separation and large turbulent wakes. The transition between hover and cruise can be made smoother and simplified since the major propulsors are fixed in the forward flight direction. Retracting flaps is a mature technology that is already widely used in aircraft, in particular if the flaps can adopt a simple configuration such as single plain flaps.

1.2 CoFlow Jet (CFJ) Active Flow Control

CFJ is a zero-net-mass-flux (ZNMF) active flow control technique recently developed by Zha and his team [6, 7, 11–24]. As illustrated in Fig. 3, a small amount of mass flow is drawn into the airfoil near the trailing edge, pressurized and energized by a micro-compressor system inside the airfoil, and then injected near the leading edge in the direction tangent to the main flow. CFJ achieves ultra-high lift coefficient exceeding the theoretical limit [6], thrust generation, and very high stall angle of attack (e.g., 70°) with low energy expenditure.

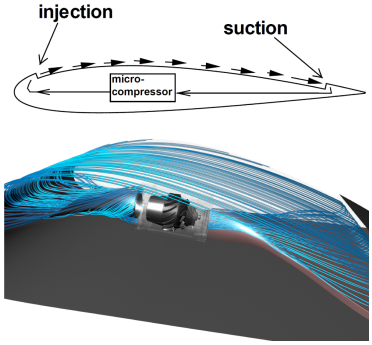

Figure 3: *CFJ airfoil concept and micro-compressor embedded.*

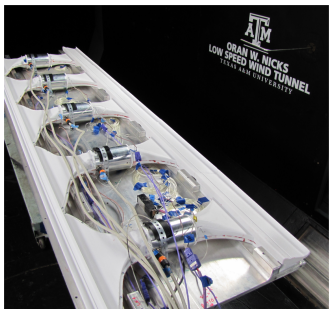

Figure 4: *Photo of the wind tunnel tested airfoil with 5 compressors embedded.*

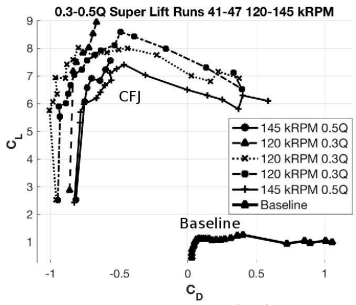

Figure 5: Measured drag polar of the CFJ and baseline airfoil [25].

Fig. 4 is the photo of the CFJ-NACA6421 airfoil recently tested in wind tunnel with 5 compressors embedded inside the airfoil along the span [25]. The C_{Lmax} of 8.6 is achieved as shown in the drag polar in Fig. 5, which is far greater than the theoretical limit of C_{Lmax}=7.6 for this airfoil. Fig. 5 also shows that the CFJ airfoil generates very high thrust up to $C_D = -1.0$. The operating range of CFJ airfoil without stall is dramatically increased. The CFJ airfoil has very low energy expenditure, which is the unique feature enabling CFJ wing to enhance productivity efficiency at cruise even when the flow is at its most favorable condition at low angle of attack [5, 8–10].

Xu et al [23, 26] analyze the mechanism of coflow wall jet and indicate that it is most efficient and effective to apply CFJ in adverse pressure gradient (APG) region, which would have the injection placed at the location of separation onset and the entire CFJ immersed in the APG area. Xu and Zha [24] apply

CFJ on an aircraft control surface flap and find that it is much more efficient and effective than applying the CFJ in the front part due to being immersed in the APG region. McBreen et al. [27] demonstrate numerically that the CFJ is able to overcome an adverse pressure gradient 3 orders of magnitude higher than the baseline configuration that has no flow control. Xu and Zha [24] conduct exergy analysis, which shows that the energy consumed by CFJ active flow control (AFC) is fully absorbed by the controlled flow as system exergy gain due to the ZNMF. The CFJ AFC is able to benefit the system efficiency attributed to the exergy benefit and improved flow performance (e.g. flow separation removal).

The purpose of this paper is to numerically demonstrate that the CoFlow Jet is feasible to deflect the slipstream of a propeller by an airfoil with a simple plain flap at low energy expenditure. This will lay a foundation for further development of the DS-CFJ technology.

1.3 Navier-Stokes Equations Solver

The in-house high order CFD code Flow-Acoustics-Structure Interaction Package (FASIP) is used to solve the 2D unsteady-Reynolds averaged Navier-Stokes equations. A 3rd order WENO scheme for the inviscid flux [28–31] and a 4th order central differencing for the viscous terms [29, 30] are employed to discretize the Navier-Stokes equations. The low diffusion E-CUSP scheme suggested by Zha et al. [31] based on the Zha-Bilgen flux vector splitting [28] is utilized with the WENO scheme to evaluate the inviscid fluxes. All the simulations in this study are conducted as unsteady time accurate simulations. The second order time-accurate implicit time marching method with pseudo time and Gauss-Seidel line relaxation is used to achieve a fast convergence rate [32, 33]. Parallel computing is implemented to save wall clock simulation time [34]. The FASIP code is intensively validated for CFJ simulations [6, 11, 13, 14, 18, 20, 22, 23, 34, 35], including the deflected slipstream with CoFlow Jet [36].

2 Results

2.1 The Design

The CFJ-NACA-6421 airfoil configuration, as illustrated in Fig. 6, features a chord length of 65 cm and was designed and tested with a flap length constituting 66.7% of the chord. The flap incorporates four Schubeler EDF DS-30-AXI (69 mm) fans embedded within it, serving as CFJ actuators. The flap deflection angle, denoted as β, is a critical parameter. At the initial hover position, aimed at redirecting the slipstream by 90°, the flap deflection angle is configured to be 78° based on CFD analysis. In the cruise configuration with the flap fully retracted, β is 0°. The flap is capable of rotating about its axis to adjust the deflection angle from 0° to 83° in this experimental setup. The propeller, with a diameter of 85.9 cm, is positioned 34.9 cm upstream of the airfoil. The black dashed line represents the initial propeller position, while the blue line indicates an alternative position tested, which is displaced upward by 1/2 of the propeller radius.

Fig. 7 shows the Mach contours with streamlines in the mid-plane of the 3D CFD simulation of the final design. The CFD result shows that the slipstream after the propeller is turned by the CFJ flap 90° downward with a flap deflection angle of 78°. Fig. 8 shows the 3D streamlines with swirl from the fan outlet in the injection duct with a centerbody to guide the flow. The inject duct cross section is changed from a circular duct to a rectangle duct to merge with the CFJ flap injection.

2.2 The Testing

The testing seeks the proof of the flow turning capability of the deflected slipstream enabled by CFJ. As shown in Fig. 9 and 10, the testing rig was built by two plexiglass walls on the two sides to form a channel with some infinite wingspan effect. The lower and upper sides are open to the air. The testing was done in the outdoor environment to mimic VTOL. Fig. 10 also shows the inner structure of the micro-fan and ducts layout.

Fig. 11 shows the hardware system tested outdoor in Hampton, Virginia, to mimic static VTOL hover condition with no freestream. Since the camera was not able to capture the fast rotating propeller blades, the propeller is invisible in the photo but is indicated by a red arrow. Fig. 11 has the CFJ turned off and the flap is deflected by 68°. Without the CFJ, the slipstream from the propeller is not able to

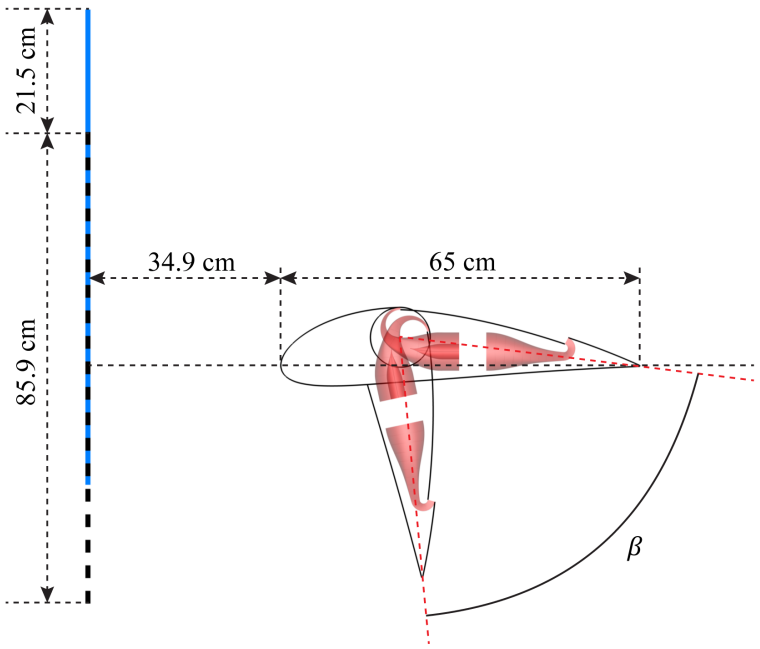

Figure 6: The CFJ-NACA-6421 airfoil configuration with a chord length of 65 cm, designed and tested.

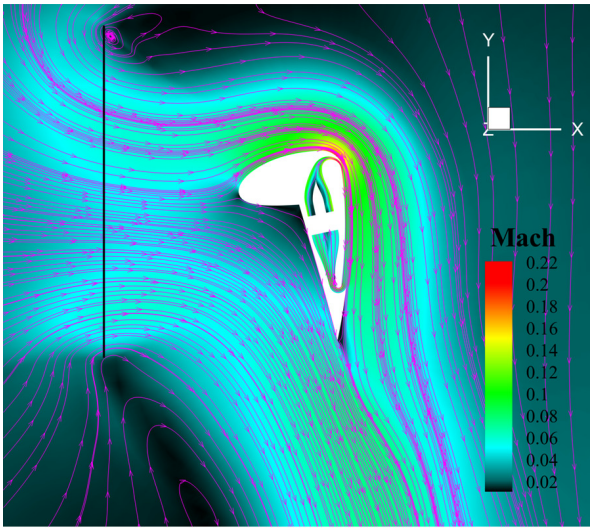

Figure 7: *Computed mid-plane Mach contours of the 3D DS-CFJ airfoil with CFJ ducts.*

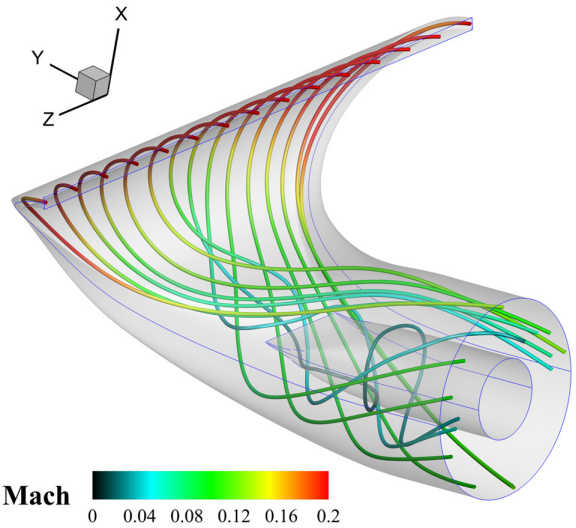

Figure 8: *Computed 3D injection duct with streamlines.*

turn and the flow goes straight downstream as shown by the smoke in Fig. 11. There is a large flow separation zone behind the flap that is not visible.

Fig. 12 shows the flow visualization with the flap deflected by 78° and the CFJ is turned on in the flap, which has 4 micro-fan actuator embedded inside. A propeller is illustrated in the front to show its position. The slipstream from the propeller is fully attached and is deflected 90° upward as shown by the smoke with red arrows showing flow direction, consistent with the measured lift and drag and the CFD simulation. Fig. 13 is the flow visualization with tufts for the same conditions of Fig. 12. Again, it shows that flow is very well attached with the flap deflected by 78°. Fig. 14 shows the tufts dropped down when the jet is turned off at the same propeller conditions as that in Fig. 11. When there CFJ is turned off, the 78° deflected flap almost acts like a vertical wall.

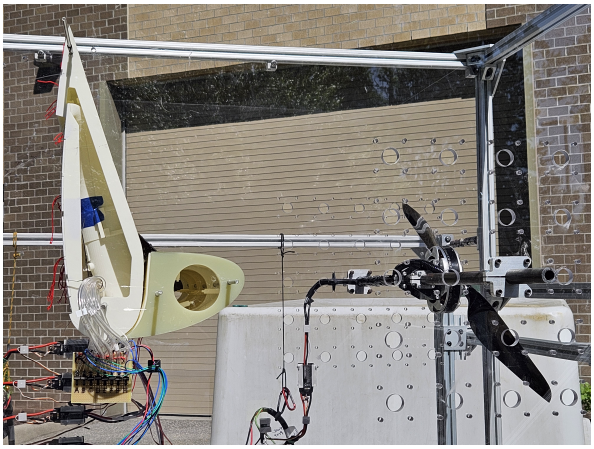

Figure 9: *Testing rig for the deflected slipstream enabled by CFJ.*

Figure 10: *Inner structure of the micro-fan and ducts layout.*

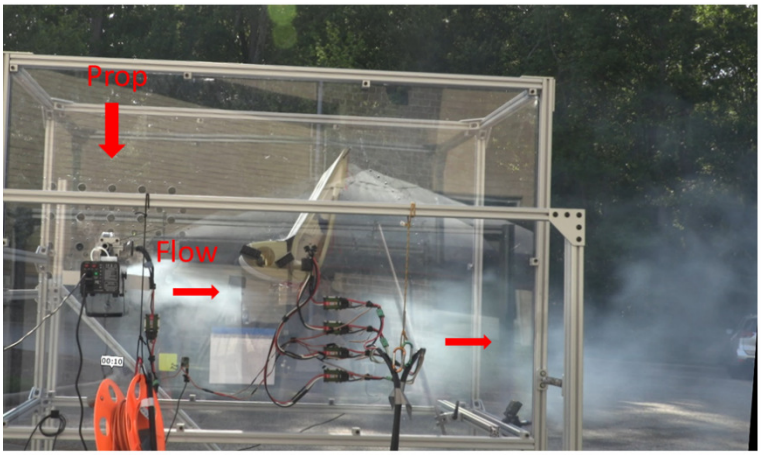

Figure 11: *Slipstream going straight downstream with CFJ off.*

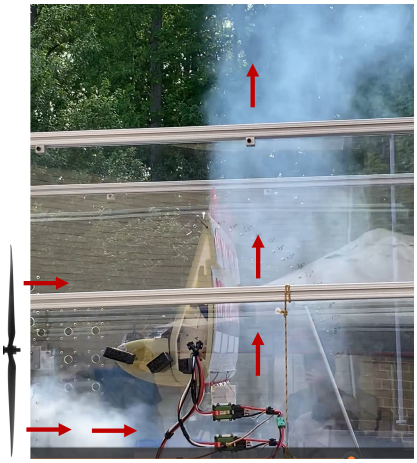

Figure 12: *Smoke showing deflected 90° by CFJ flap at 78° during testing.*

Figure 13: *Tufts showing slipstream deflected 90° by CFJ flap at 78° during testing.*

Figure 14: *Tufts drop down when the jet is turned off.*

Fig. 15 presents the quantitative measurements of lift, thrust, and resultant force angle at a flap deflection angle of 78°. The first column displays results with the propeller in its original position with the propeller center aligned with the airfoil leading edge, while the second column shows results with

the propeller moved up by 1/2 of the propeller radius. The first, second, and third rows correspond to the measurements of lift, thrust, and resultant force angles, respectively. These measurements were taken across a range of propeller power settings from 20% to 100%, and CFJ fan actuator power settings from 0% to 100%. A CFJ fan actuator power setting of 0% indicates that the CFJ system is turned off.

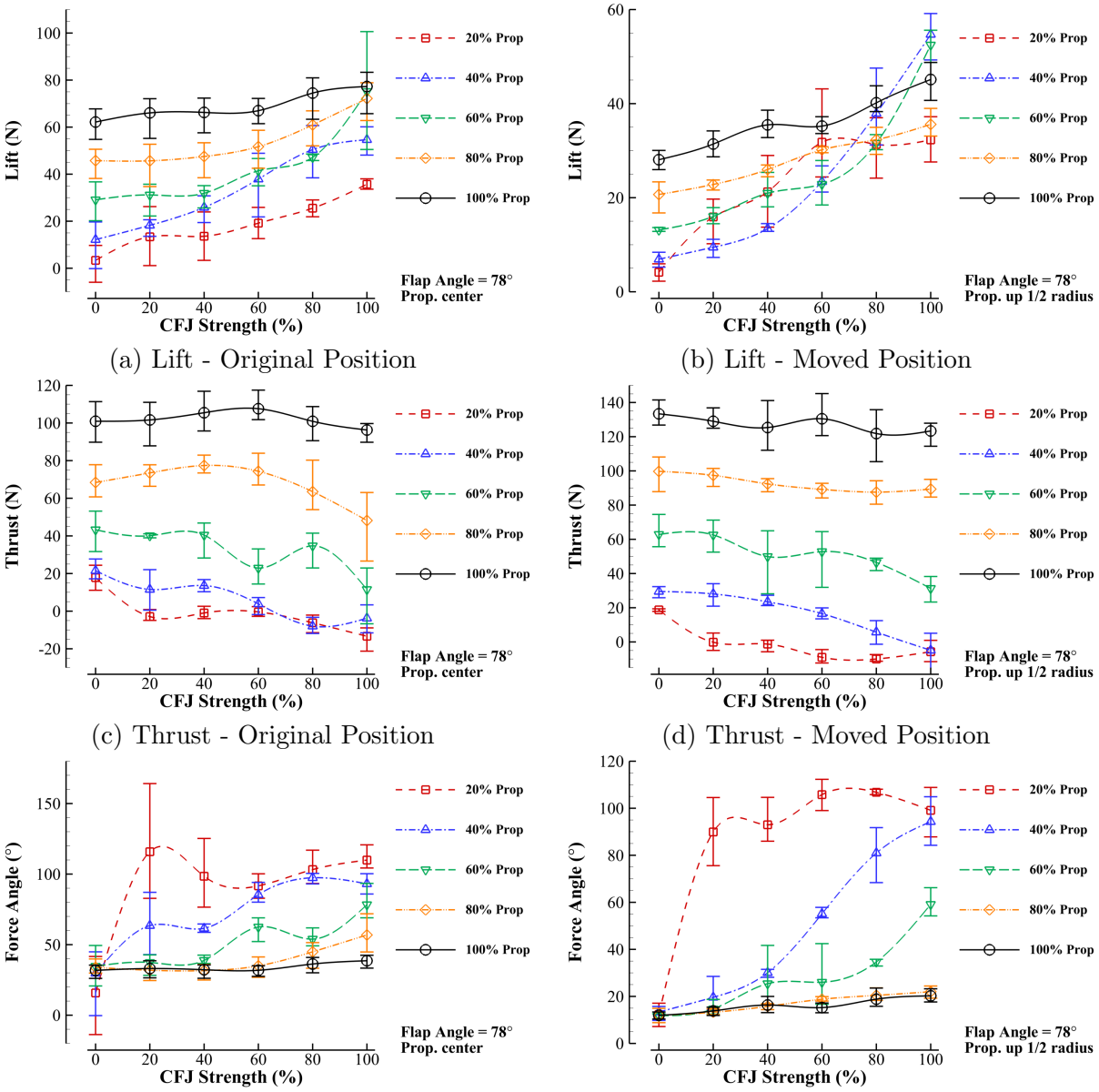

(a) Lift - Original Position

(b) Lift - Moved Position

(c) Thrust - Original Position

(d) Thrust - Moved Position

(e) Resultant Force Angle - Original Position

(f) Resultant Force Angle - Moved Position

Figure 15: Quantitative measurements of lift, thrust, and resultant force angle at a flap deflection angle of 78°, with varying propeller and CFJ fan actuator power settings.

Fig. 15 (e) and (f) indicate that when the CFJ is deactivated, the flow turning is minimal, with the slipstream deflection angle ranging between 10° and 30°. This limited deflection is due to massive flow separation behind the flap, causing the slipstream to move predominantly straight downstream, as depicted in Fig. 11. When the CFJ fan power is activated at 20%, the flow deflection increases significantly, reaching up to 120° at a propeller power of 20%. As the CFJ power is further increased to 100%, the slipstream deflection angle fluctuates between 90° and 120°. At a propeller power of 40%, the flow turns 90° when the CFJ power is at 80% or higher. The use of off-the-shelf micro-fans results in a power mismatch with the propeller, whereby the micro-fans' power is insufficient to match and turn

the flow when the propeller power is too high. Nevertheless, at lower propeller power settings, the tests demonstrate that the flapped CFJ airfoil is capable of achieving flow deflection angles of 90° or greater. When the deflection angle exceeds 90°, the airfoil experiences a backward force. This experimental investigation confirms the high effectiveness of the deflected slipstream technique enabled by CFJ in controlling the flow.

For the case with the propeller moved up by 1/2 of the propeller radius (Fig. 15 (b), (d), (f)), the force angles exhibit similar behavior when the propeller strength is at 20%. However, at higher propeller strengths, the CFJ strength becomes more sensitive compared to the original position case. This heightened sensitivity results in a more pronounced distinction between separated and attached flow regimes, thereby enhancing the effectiveness of flow control.

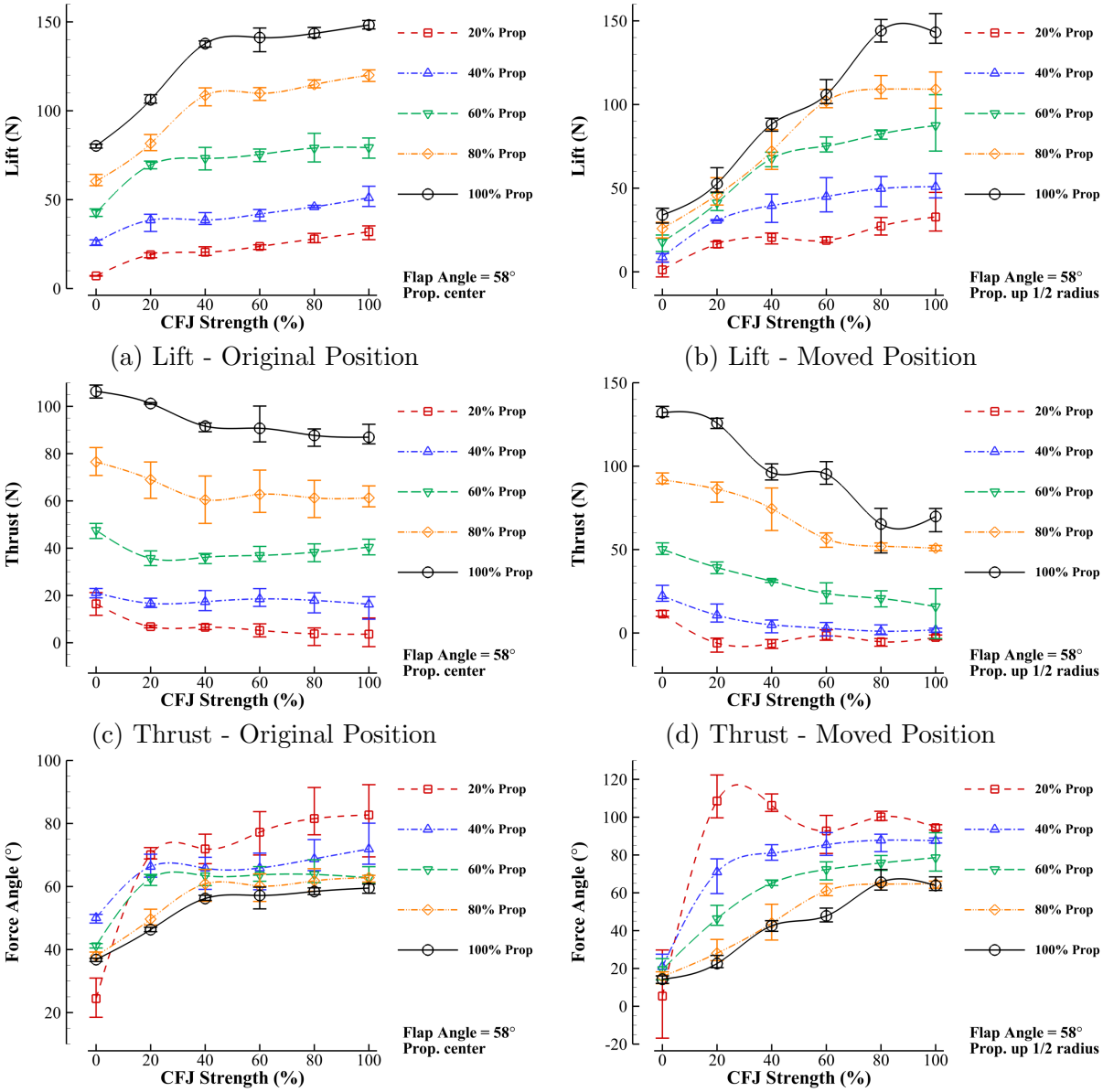

(a) Lift - Original Position

(b) Lift - Moved Position

(c) Thrust - Original Position

(d) Thrust - Moved Position

(e) Resultant Force Angle - Original Position

(f) Resultant Force Angle - Moved Position

Figure 16: Quantitative measurements of lift, thrust, and resultant force angle at a flap deflection angle of 58°, with varying propeller and CFJ fan actuator power settings.

Fig. 16 presents the quantitative measurements of lift, thrust, and resultant force angle at a flap deflection angle of 58°. For this case, the case with the propeller moved up (Fig. 16 (b), (d), (f)) show

much greater turning angle (force) compared to the original position with the propeller centered to the airfoil. When the flow is nicely attached, the results indicate larger lift, smaller thrust, and larger force angles compared to the original propeller position case. Moving the propeller up can enhance the wake turning and improve the efficiency of the DS-CFJ system by facilitating better flow attachment and increasing the effectiveness of flow control.

2.3 Future Improvement

The testing seeks the initial proof of the concept for deflected slipstream enabled by CoFLow Jet. However, the CFJ is not not effectively implemented and it is difficult to have accurate assessment of the CFJ performance efficiency for several reasons: 1) Due to the limitation of a low budget, the 3D printed CFJ airfoil and its ducts had a leak of the CFJ air in the testing; 2) The CFJ fans selected are off-the-shelf products and the pressure ratio is about 1.04, which is too low to match the high strength of the slipstream when the propeller is at full power considering the pressure loss in the suction and injection ducts. The leak of the CFJ airfoil further weakens the CFJ effectiveness. 3) Since the characteristics of the fan and geometry are unknown, we can not design the duct to match the fan flow profile. In the testing, it is observed that the flow at the CFJ injection is quite non-uniform with the injection jet much stronger on the two side walls of the slot outlet and weak in the middle of the slot. It can be due to the swirl effect of the fan outlet flow and also can be caused by the 3D printed ducts deformation.

However, even though these effects weakened the CFJ effectiveness, the testing still demonstrates the effectiveness of the turning of the DS enabled by CFJ. These weaknesses actually provide a lot of room for future improvement.

3 Summary

This study presents the design and testing of a Deflected Slipstream (DS) airfoil, enabled by CoFlow Jet (CFJ) active flow control. The focus is on VTOL hover applications. Through numerical simulations and experimental tests, we demonstrated the ability of the CFJ-NACA-6421 airfoil to achieve significant flow deflection and improved aerodynamic performance. The results showed that the use of CFJ actuators effectively enhances the flow attachment and increases the deflection angles beyond the flap deflection angles, thereby proving the high effectiveness of the DS-CFJ system. The analysis covered various configurations, including different propeller positions and flap angles, highlighting the impact on lift, thrust, and resultant force angles. The findings indicate that adjusting the propeller position can enhance wake turning and overall system efficiency. These insights provide a foundation for further optimization and potential application of the DS-CFJ technology in future VTOL aircraft designs.

4 Acknowledgment

This study was supported by NASA Langley Research Center under contracts 80LARC20F0095/NIA.IDIQC.03.602005 and 80LARC17C0004/NIA.COOP.05.201070 with the National Institute of Aerospace. The author would like to acknowledge Siena K. S. Whiteside and Paul M. Rothhaar of NASA Langley Research Center for their technical contributions and leadership.

References

[1] K. R. Antcliff, S. K. Whireside, L. W. Kohlman, and C. Silva, "Baseline Assumptions and Future Research Areas for Urban Air Mobility Vehicles." AIAA Paper 2019-0528, AIAA SciTech 2019 Forum, San Diego, CA, 7-11 January 2019.

[2] R. E. Kuhn and J. W. Draper, "An Investigation of a Wing-Propeller configuration Employing Large-Chord Plain Flaps and Large-Diameter Propellers for Low-Speed Flight and Vertical Take-Off ." NACA TN-3307, December 1954.

[3] R. E. Kuhn and J. W. Draper, "Investigation of Effectiveness of Large-Chord Slotted Flaps in Deflecting Propeller Slipstreams Downward for Vertical Take-Off and Low-Speed Flight ." NACA TN-3364, Jan. 1955.

[4] R. E. Kuhn, "Investigation of the Effects of Ground Proximity and Propeller Position on the Effectiveness of a Wing with Large-Chord Slotted Flaps in Redirecting Propeller Slipstreams Downward for Vertical Take-Off ." NACA TN-3629, March 1956.

[5] Lefebvre, A. and Zha, G.-C., "Trade Study of 3D Co-Flow Jet Wing for Cruise and Takeoff/Landing Performance." AIAA Paper 2016-0570, AIAA SCITECH2016, AIAA Aerospace Science Meeting, San Diego, CA, 4-8 January 2016.

[6] Yang, Y.-C. and Zha, G.-C., "Super-Lift Coefficient of Active Flow Control Airfoil: What Is the Limit?." AIAA Paper 2017-1693, AIAA SCITECH2017, 55th AIAA Aerospace Science Meeting, Grapevine, Texas, 9-13 January 2017.

[7] Lefebvre, A. and Zha, G.-C. , "Design of High Wing Loading Compact Electric Airplane Utilizing Co-Flow Jet Flow Control." AIAA Paper 2015-0772, AIAA SciTech2015: 53rd Aerospace Sciences Meeting, Kissimmee, FL, 5-9 Jan 2015.

[8] Y. Wang and G.-C. Zha, "Study of 3D Co-flow Jet Wing Induced Drag and Power Consumption at Cruise Conditions." AIAA Paper 2019-0034, AIAA SciTech 2019, San Diego, CA, January 7-11, 2019.

[9] Y. Wang, Y.-C. Yang, and G.-C. Zha, "Study of Super-Lift Coefficient of Co-Flow Jet Airfoil and Its Power Consumption." AIAA Paper 2019-3652, AIAA Aviation 2019, AIAA Applied Aerodynamics Conference, Dallas, Texas, 17-21 June 2019.

[10] Yang, Y.-C. and Zha, G.-C., "Numerical Investigation of Performance Improvement of the Co-Flow Jet Electric Airplane." AIAA Paper 2018-4208, AIAA AVIATION Forum 2018, 2018 Applied Aerodynamics Conference, Atlanta, Georgia, June 25-29, 2018.

[11] Zha, G.-C. and Gao, W. and Paxton, C., "Jet Effects on Co-Flow Jet Airfoil Performance," *AIAA Journal, No. 6,*, vol. 45, pp. 1222–1231, 2007.

[12] G.-C. Zha and D. C. Paxton, "A Novel Flow Control Method for Airfoil Performance Enhancement Using Co-Flow Jet." *Applications of Circulation Control Technologies*, Chapter 10, p. 293-314, Vol. 214, Progress in Astronautics and Aeronautics, AIAA Book Series, Editors: Joslin, R. D. and Jones, G.S., 2006.

[13] Zha, G.-C and Paxton, C. and Conley, A. and Wells, A. and Carroll, B., "Effect of Injection Slot Size on High Performance Co-Flow Jet Airfoil," *AIAA Journal of Aircraft*, vol. 43, 2006.

[14] Zha, G.-C and Carroll, B. and Paxton, C. and Conley, A. and Wells, A., "High Performance Airfoil with Co-Flow Jet Flow Control," *AIAA Journal*, vol. 45, 2007.

[15] Wang, B.-Y. and Haddoukessouni, B. and Levy, J. and Zha, G.-C., "Numerical Investigations of Injection Slot Size Effect on the Performance of Co-Flow Jet Airfoil ," *AIAA Journal of Aircraft*, vol. 45, pp. 2084–2091, 2008.

[16] B. P. E. Dano, D. Kirk, and G.-C. Zha, "Experimental Investigation of Jet Mixing Mechanism of Co- Flow Jet Airfoil." AIAA-2010-4421, (5th AIAA Flow Control Conference, Chicago, IL), 28 Jun - 1 Jul 2010.

[17] B. P. E. Dano, G.-C. Zha, and M. Castillo, "Experimental Study of Co-Flow Jet Airfoil Performance Enhancement Using Micro Discreet Jets." AIAA Paper 2011-0941, 49th AIAA Aerospace Sciences Meeting, Orlando, FL,, 4-7 January 2011.

[18] Lefebvre, A. and Dano, B. and Bartow, W. and Di Franzo, M. and Zha, G.-C., "Performance and Energy Expenditure of Co-Flow Jet Airfoil with Variation of Mach Number," *AIAA Journal of Aircraft*, vol. 53, pp. 1757–1767, 2016.

[19] Lefebvre, A. and Zha, G.-C., "Numerical Simulation of Pitching Airfoil Performance Enhancement Using Co-Flow Jet Flow Control." AIAA Paper 2013-2517, AIAA Applied Aerodynamics Conference, San Diego, CA, 24 - 27 June 2013.

[20] Liu, Z.-X. and Zha, G.-C., "Transonic Airfoil Performance Enhancement Using Co-Flow Jet Active Flow Control." AIAA Paper 2016-3472, AIAA AVIATION 2016, 8th AIAA Flow Control Conference, Washington, D.C, June 13-17, 2016.

[21] K.-W. Xu and G.-C. Zha, "High control authority 3d aircraft control surfaces using co-flow jet," *AIAA Journal of Aircraft*, July 2020.

[22] Xu, Kewei and Zha, Gecheng, "System energy benefit using co-flow jet active separation control for a serpentine duct," *Elsevier Journal of Aerospace Science and Technology*, vol. 128, p. DOI: 10.1016/j.ast.2022.107746, 2022.

[23] Xu, Kewei and Ren, Yan and Zha, Gecheng, "Numerical Analysis of Energy Expenditure for Co-Flow Wall Jet Separation Control ," *AIAA Journal*, vol. 60, no. 5, p. doi.org/10.2514/1.J061015, 2022.

[24] Xu, Kewei and Zha, Gecheng, "Enhancing aircraft control surface effectiveness by co-flow jet flap at low energy expenditure ," *Elsevier Journal of Aerospace Science and Technology*, vol. 133, 2023.

[25] G.-C. Zha, Y.-C. Yang, Y. Ren, and B. McBreen, "Super-lift and thrusting airfoil of coflow jet-actuated by micro-compressors." AIAA Paper 2018-3061, AIAA AVIATION 2018, Atlanta, GA , 25 - 29 June 2018.

[26] K.-W. Xu, Y. Ren, and G.-C. Zha, "Flow separation control by coflow wall jet." AIAA Paper 2021-2946, AIAA Aviation 2021, Virtual Events, Submitted to AIAA Journal, 2-6 Aug. 2021.

[27] McBreen, B. and Xu, K.-W. and Zha, G.-C., "Numerical Study of Extreme Adverse Pressure gradients Enabled by Co-Flow Jet." AIAA Paper 2023-1430, AIAA 2023 SciTech Forum, National Harbor, MD , 23-27 Jan. 2023.

[28] G.-C. Zha and E. Bilgen, "Numerical Solutions of Euler Equations by Using a New Flux Vector Splitting Scheme ," *International Journal for Numerical Methods in Fluids*, vol. 17, pp. 115–144, 1993.

[29] Shen, Y.-Q. and Zha, G.-C. and Chen, X.-Y., " High Order Conservative Differencing for Viscous Terms and the Application to Vortex-Induced Vibration Flows," *Journal of Computational Physics*, vol. 228(2), pp. 8283–8300, 2009.

[30] Y.-Q. Shen and G.-C. Zha, "Large Eddy Simulation Using a New Set of Sixth Order Schemes for Compressible Viscous Terms ," *Journal of Computational Physics*, vol. 229, pp. 8296–8312, 2010.

[31] G.-C. Zha, Y. Shen, and B. Wang, "An improved low diffusion E-CUSP upwind scheme ," *Journal of Computer & Fluids*, vol. 48, pp. 214–220, 2011.

[32] G. C. Zha, D. Smith, M. Schwabacher, K. Rasheed, A. Gelsey, and D. Knight, "High Performance Supersonic Missile Inlet Design Using Automated Optimization." AIAA Paper 96-4142, 1996.

[33] X.-Y. Chen and G.-C. Zha, "Fully Coupled Fluid-Structural Interactions Using an Efficient High Solution Upwind Scheme." AIAA Paper 2004-2331, to appear in Journal of Fluids and Structures, 2005.

[34] B.-Y. Wang and G.-C. Zha, "A General Sub-Domain Boundary Mapping Procedure For Structured Grid CFD Parallel Computation," *AIAA Journal of Aerospace Computing, Information, and Communication*, vol. 5, No.11, pp. 2084–2091, 2008.

[35] K.-W. Xu and G.-C. Zha, "Mitigation of Serpentine Duct Flow Distortion Using CoFlow Jet Active Flow Control ." AIAA-2020-2954, AIAA Aviation 2020 Virtual Forum, 15-19 June, 2020.

[36] G.-C. Zha, "Feasibility Study of Deflected Slipstream Airfoil for VTOL Hover Enabled by CoFlow Jet." AIAA Paper 2023-4279, AIAA Aviation Forum 2023, San Diego, CA, 12-16 June 2023.